

## REGIONAL BLOOD VOLUME IN FRONTAL CORTEX DURING NREM SLEEP: A NIRS STUDY

## A Biphasic Change of Regional Blood Volume in the Frontal Cortex during Non-Rapid Eye Movement Sleep: A Near-Infrared Spectroscopy Study

Zhongxing Zhang, PhD<sup>1,2</sup>; Ramin Khatami, MD<sup>1,2,3</sup><sup>1</sup>Center for Sleep Medicine and Sleep Research, Clinic Barmelweid, Barmelweid, Switzerland; <sup>2</sup>Department of Neurology, University Hospital Bern, Bern, Switzerland; <sup>3</sup>ZIHP, Zurich Center for Integrative Human Physiology, Zürich, Switzerland

**Study Objectives:** Current knowledge on hemodynamics in sleep is limited because available techniques do not allow continuous recordings and mainly focus on cerebral blood flow while neglecting other important parameters, such as blood volume (BV) and vasomotor activity.

**Design:** Observational study.

**Participants and Settings:** Continuous measures of hemodynamics over the left forehead and biceps were performed using near-infrared spectroscopy (NIRS) during nocturnal polysomnography in 16 healthy participants in sleep laboratory.

**Measurements and Results:** Temporal dynamics and mean values of cerebral and muscular oxygenated hemoglobin (HbO<sub>2</sub>), deoxygenated hemoglobin (HHb), and BV during different sleep stages were compared. A biphasic change of cerebral BV was observed which contrasted a monotonic increase of muscular BV during non-rapid eye movement sleep. A significant decrement in cerebral HbO<sub>2</sub> and BV accompanied by an increase of HHb was recorded at sleep onset (Phase I). Prior to slow wave sleep (SWS) HbO<sub>2</sub> and BV turned to increase whereas HHb began to decrease in subsequent Phase II suggested increased brain perfusion during SWS. The cerebral HbO<sub>2</sub> slope correlated to BV slope in Phase I and II, but it only correlated to HHb slope in Phase II. The occurrence time of inflection points correlated to SWS latencies.

**Conclusion:** Initial decrease of brain perfusion with decreased blood volume (BV) and oxygenated hemoglobin (HbO<sub>2</sub>) together with increasing muscular BV fit thermoregulation process at sleep onset. The uncorrelated and correlated slopes of HbO<sub>2</sub> and deoxygenated hemoglobin indicate different mechanisms underlying the biphasic hemodynamic process in light sleep and slow wave sleep (SWS). In SWS, changes in vasomotor activity (i.e., increased vasodilatation) may mediate increasing cerebral and muscular BV.

**Keywords:** cerebral blood volume, sleep onset, vasodilatation

**Citation:** Zhang Z, Khatami R. A biphasic change of regional blood volume in the frontal cortex during non-rapid eye movement sleep: a near-infrared spectroscopy study. *SLEEP* 2015;38(8):1211–1217.

## INTRODUCTION

Changes in cerebral hemodynamics are important for understanding the function of sleep and the pathophysiology of sleep disorders including cardiovascular diseases, because hemodynamics carries information about metabolism, neuronal functioning, vasomotor activity, and temperature.<sup>1–3</sup> The most important factors contributing to cerebral hemodynamics include blood volume (BV), cerebral blood flow (CBF), vasoconstriction/vasodilatation, oxygenated (HbO<sub>2</sub>) and deoxygenated (HHb) hemoglobin, and oxygen saturation. Currently most human sleep studies using functional magnetic resonance imaging (fMRI),<sup>2,4</sup> positron emission tomography (PET)<sup>2,5–7</sup> and transcranial Doppler (TCD)<sup>8,9</sup> referred to CBF changes only but did not evaluate the other parameters. Reduced glucose utilization and CBF velocity during sleep onset have been reported,<sup>2,5,6,9</sup> suggesting decreased cerebral perfusion during sleep initiation. However, CBF changes alone cannot provide sufficient information of cerebral perfusion because BV depends on both CBF velocity and vessel diameter.<sup>10,11</sup> Velocity can be used as an index of flow only under the assumption that the vessel diameter does not change.<sup>8,10</sup> Recent studies have challenged this assumption in TCD measurements by showing

increased vessel diameter during hypercapnia.<sup>10,12</sup> The influence of vasomotor activity on local cerebral perfusion in sleep is still far from clear because of methodological limits of available techniques such as the low temporal resolution of PET.<sup>2,6</sup> Changes of vasomotor mediators such as increasing partial pressure of carbon dioxide in arterial blood (PaCO<sub>2</sub>) have been reported after falling asleep.<sup>13</sup> Interestingly, all characterized sleep regulatory substances that can enhance sleep are cerebral vasodilators.<sup>14,15</sup> How the changes of vasodilation and CBF velocity influence cerebral BV during natural human sleep is still unknown.

Furthermore, the aforementioned neuroimaging techniques cannot provide information on hemodynamics of peripheral tissues such as skin and muscle. Peripheral hemodynamic changes during sleep initiation are tightly coupled with thermoregulation. Increasing skin temperature and perfusion at sleep onset is a well-known mechanism to modulate heat loss to initiate sleep.<sup>3,16,17</sup> Thus, simultaneous measures of peripheral and cerebral hemodynamics can provide complementary insights into the underlying mechanisms of sleep and allow us to test whether the changing pattern of cerebral hemodynamics is specific for the brain due to cerebral autoregulation mechanisms and neurovascular coupling or coupled to systemic changes. Therefore, a novel neuroimaging technique that can measure multihemodynamic parameters in local cerebral and peripheral tissues in natural human sleep with high temporal resolution is needed.

Near-infrared spectroscopy (NIRS) is a totally non-invasive and non-radiation optical method that can measure changes of local intravascular oxygen saturation, HbO<sub>2</sub>, HHb, and BV with less motion restriction.<sup>18,19</sup> Previous studies have conducted

Submitted for publication July, 2014

Submitted in final revised form December, 2014

Accepted for publication January, 2015

Address correspondence to: Ramin Khatami, MD, Center for Sleep Medicine and Sleep Research, Clinic Barmelweid, 5017 Barmelweid, Switzerland; Tel: +41 062 857 2228; Fax: +41062 857 2225; Email: ramin.khatami@barmelweid.ch

cerebral NIRS measurements during sleep in healthy people and patients with sleep disorders,<sup>19–23</sup> within which only very few studies described cerebral hemodynamics during the sleep onset process. Decrements in cerebral HbO<sub>2</sub> and cerebral BV after sleep initiation were observed with NIRS.<sup>22,23</sup> Hoshi et al. suggested that these decrements may indicate increased oxygen metabolic rate during sleep initiation.<sup>22</sup> By contrast, Spielman et al. proposed that decreased cerebral BV and HbO<sub>2</sub> may reduce oxygen consumption and neuronal activity during sleep initiation.<sup>23</sup> The conflicting conclusions cannot be explained without taking peripheral hemodynamics into account, but neither of these two studies considered the contrast from peripheral hemodynamics. Also, their results should be treated with caution given the potential artefacts arising from skin blood, because both groups used single-channel NIRS instruments, which are unable to differentiate skin from brain perfusion.<sup>2,24</sup>

Therefore, we investigated the cerebral and muscular hemodynamics simultaneously with multi-channel NIRS that can well eliminate superficial influences.<sup>24</sup> We hypothesized that muscular BV may increase during sleep initiation under the control of increasing vasodilatation (mediated by vasodilator, e.g. PaCO<sub>2</sub><sup>13</sup>) according to the well-known thermoregulation process,<sup>3,16,17</sup> whereas cerebral BV will show different patterns due to the influences of unique cerebral mechanisms such as cerebral vascular autoregulation and sleep related neuronal activities. A better understanding of BV changes will close the gap between the changes of local cerebral CBF and vasodilatation reported by previous studies; moreover, the comparisons of BV, HbO<sub>2</sub>, and HHb changes between the brain and muscle can improve our understanding of metabolic changes during sleep onset.

## METHODS

### Subjects

Sixteen healthy volunteers (eight males, eight females, age  $30 \pm 9.9$  y [mean  $\pm$  standard deviation] ) participated in this study at Center for Sleep Medicine and Sleep Research, Clinic Barmelweid, Switzerland. The study was approved by the local ethics committee, and all subjects gave their written informed consent to participate into the study. Three measurements (two males and one female) were excluded from the subsequent data analysis due to the poor quality of NIRS data. None of the subjects has any sleep disorders, ischemic heart disease, chronic heart failure, or cerebrovascular disorders.

### Video-Polysomnography Measurement

A polysomnography (PSG) (Embla RemLogic, Embla Systems LLC, Tonawanda, NY, USA) consisting of electroencephalography (EEG, channels F4-A1, C4-A1, O2-A1, F3-A2, C3-A2, and O1-A2), left and right electrooculography, chin and two-leg electromyography was recorded from all subjects. Peripheral arterial oxygen saturation was measured with a fingertip pulse oximeter (sample rate: 10 Hz), and heart rate could also be derived from the same measurement by calculating the peak-to-peak pulsation interval of the measured photoplethysmographic waveform. During the measurements, the subjects were videotaped with an infrared camera to allow for subsequent assessment of subject's movement. Based on the PSG

measures, a full experienced neurophysiologist independently scored the sleep into stages N1, N2, slow wave sleep (SWS), rapid eye movement (REM) sleep, wakefulness (W), and movement time stages in 30-sec epochs according to the American Academy of Sleep Medicine scale.<sup>25</sup> If two similarly scored 30-sec epochs were separated by one 30-sec epoch scored differently, that epoch was rescored to match its surroundings. Then another experienced neurophysiologist double-checked the score results independently. The differences between these two independent score results were further corrected by these two neurophysiologists working together.

### NIRS Measurement

A commercialized NIRS device (NIRO-300, Hamamatsu Photonics, Japan) based on spatially resolved spectroscopy was used to monitor the hemodynamic changes during sleep monitoring.<sup>26</sup> NIRO-300 used four wavelengths of near-infrared light (775, 810, 850, and 910 nm). The optical probe contained one light emitter and three closely placed sensors (i.e., an integrated three-segment photodiode chip with the separation of 1 mm). The distance between emitter and the center of the integrated photodiode chip is 4 cm. All the sensors can pick up photons penetrating into superficial and deep tissues, but the photons reaching to far-end sensor can go approximately 3 mm deeper.<sup>27</sup> Therefore, NIRO-300 can calculate the change in light intensity over distance and remove the influence of superficial tissue (please refer to the literature<sup>26</sup> describing the design of NIRO-300) and consequently is more sensitive to the deep tissue such as cortex and muscle. NIRO-300 can locally measure relative HbO<sub>2</sub> and HHb changes by calculating the light attenuation changes in tissue based on modified Beer-Lambert law.<sup>18</sup> It can evaluate the tissue oxygen saturation changes by measuring the quantitative data of tissue oxygen index which was the ratio of HbO<sub>2</sub> to total haemoglobin. In this study, one of the NIRO-300 probes was kept in good contact with the left side of the subject's forehead, just below the hairline and above the left brow, via a medical adhesive. The second NIRO-300 probe was attached to the left bicep brachii muscle via the same way. The sample rate of NIRS measurement was 1 Hz. The raw analog outputs of NIRO-300 measurements were sampled by the data acquisition system of video-PSG, so that NIRS and PSG measurements were synchronized.

### Protocol

All the subjects came to the Center for Sleep Medicine and Sleep Research at Clinic Barmelweid between 20:00 pm and 21:00. After wearing all the PSG and NIRS probes (at around 21:30 to 22:00), the subjects were asked to stay in the bed. All the subjects began to fall asleep before 23:30, and waken up at around 07:00.

### Data Analysis

All data were expressed as means  $\pm$  standard error (SE) unless indicated otherwise. Only solid changing trends of NIRS data during the first sleep cycle that meet the following criteria were chosen: data without motion artifact, and stable sleep stages (i.e., no transitions between different sleep stages). Selected NIRS data were filtered by a low-pass filter (type II Chebyshev filter, passband edge is 150 mHz) to further eliminate

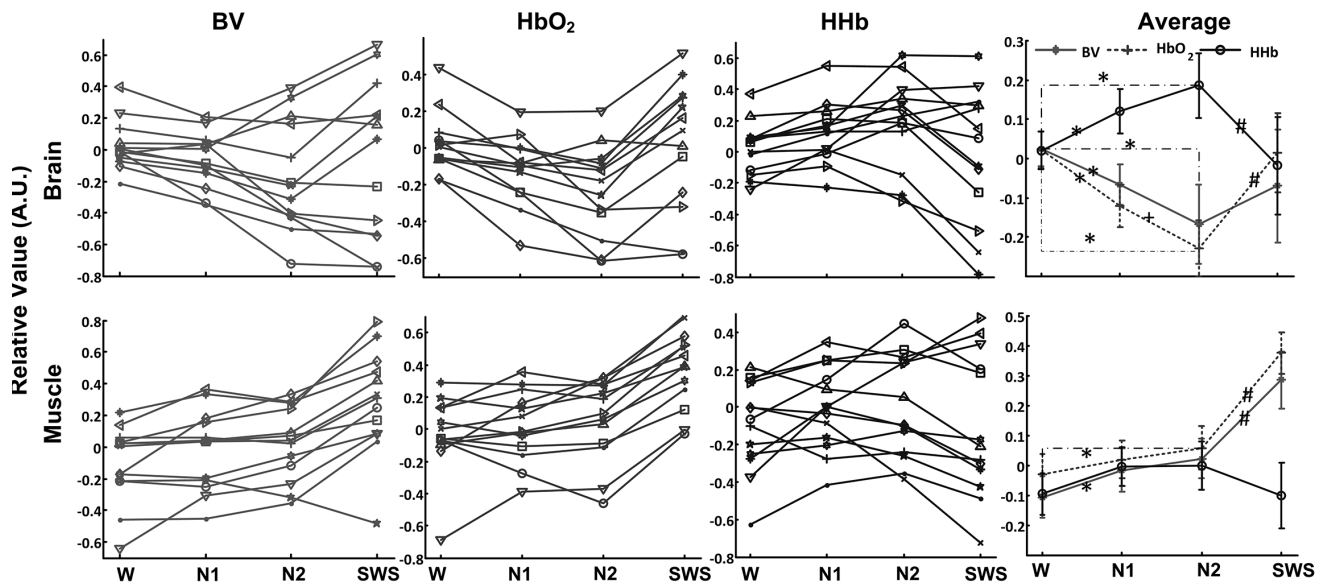


**Figure 1**—The mean cerebral and muscular hemodynamic values during different sleep stages in all subjects. BV is blood volume. \*Significant decline (or increment) in the mean hemodynamic values in sleep stage 1 (N1) and 2 (N2) compared to wakefulness (W) ( $P < 0.05$ ). #Significant decrement from N1 to N2. #Significant increment or decrement from N2 to SWS. The hemodynamic changes are expressed in arbitrary units (A.U.), as the mean value of first 30-sec measurements during wakefulness is set at 0.

the oscillations related to respiration. As individual length of selected sleep stages considerably varied between different subjects, we chose to compare the mean hemodynamic values of each sleep stage. The mean NIRS signals ( $\text{HbO}_2$ , HHb, and BV) values during W, N1, N2, and SWS were subjected to one way repeated-measures analysis of variance (ANOVA) with least significant difference (LSD) *post hoc* test ( $P < 0.05$ ), respectively. Mauchly test was used to test the assumption of sphericity ( $P < 0.05$ ). Degrees of freedom were corrected using Greenhouse-Geisser (or Huynh-Feldt) correction if the Greenhouse-Geisser estimate of sphericity was smaller (or larger) than 0.75, but original degrees of freedom were reported for sake of readability. The changing trends of NIRS signals were fitted with polynomial curve fitting (degree  $n = 20$ ), and the nadir/peak of the fitted curves were identified as the inflection points (IPs) automatically. Paired *t*-test was used to compare the latencies of NIRS IPs and SWS latencies (calculated as the time interval between the start points of N1 and SWS) ( $P < 0.05$ ), and Pearson correlation was used to test their correlations ( $P < 0.05$ ). Raw NIRS data during sleep before and after inflection points were fitted linearly, respectively, and the slopes were compared with Pearson correlation ( $P < 0.05$ ). All signal preprocessing was carried out in MATLAB (The MathWorks, Inc., Natick, MA, USA). All statistical analyses were performed using SPSS Statistics 17.0 (IBM Corporation, USA) computer programs.

## RESULTS

### Hemodynamic Changes in Different Sleep Stages

The mean cerebral and muscular hemodynamic values during different sleep stages in all subjects are illustrated in Figure 1. In a majority of subjects mean cerebral  $\text{HbO}_2$  and BV values decrease after entering light sleep (includes N1 and

N2) and they turn to increase in SWS; whereas cerebral HHb shows a reversed changing trend (upper panels in Figure 1). Statistical analysis only finds significant main effects of sleep stages for cerebral  $\text{HbO}_2$  ( $F(3,36) = 8.25$ ,  $P = 0.04$ ), but not for BV ( $F(3,36) = 1.78$ ,  $P = 0.2$ ) or HHb ( $F(3,36) = 2.92$ ,  $P = 0.1$ ). Pairwise *post hoc* comparisons reveal that the mean cerebral  $\text{HbO}_2$  value continues to decrease from wakefulness to N2 ( $P < 0.05$ ), and significantly increases ( $P < 0.05$ ) in SWS. Cerebral HHb significantly increases after entering into sleep while turns to decrease in SWS ( $P < 0.05$ ). The declines in cerebral BV can also be observed from wakefulness to N2, but there is no significant increment from N2 to SWS ( $P = 0.171$ ).

In muscle measurements (lower panels in Figure 1)  $\text{HbO}_2$  is relative constant after entering into light sleep, whereas BV and HHb increase in most of the subjects. Muscular  $\text{HbO}_2$  and BV increase while HHb declines in SWS. Statistical analysis reveals significant main effects in BV ( $F(3,36) = 20.74$ ,  $P < 0.001$ ) and  $\text{HbO}_2$  ( $F(3,36) = 34.2$ ,  $P < 0.001$ ) measurements, but not in HHb ( $F(3,36) = 1.34$ ,  $P = 0.28$ ) changes. *Post hoc* tests show increasing BV in N1 and N2 compared to wakefulness ( $P < 0.05$ ) with a further increase of BV in SWS and strong increments in  $\text{HbO}_2$  from N2 to SWS.

### The Inflection Points of Cerebral NIRS Signals and the Latencies of SWS

An example of the identification of IPs of cerebral  $\text{HbO}_2$  is illustrated in Figure 2, and the time point corresponding to the IPs in cerebral hemodynamics in all subjects is summarized in Table 1. The IPs can be identified in all subjects (except from HHb changes in subject No. 2), and they occur at  $7.95 \pm 1.02$  ( $n = 13$ ),  $8.40 \pm 1.26$  ( $n = 12$ ) and  $8.40 \pm 1.40$  ( $n = 13$ ) min after falling asleep in cerebral  $\text{HbO}_2$ , HHb and BV, respectively. The occurrence time of IPs of cerebral  $\text{HbO}_2$  is earlier than the SWS latencies ( $10.44 \pm 1.36$  min) ( $P = 0.02$ ), and they

are highly correlated ( $r^2 = 0.732$ ,  $P = 0.004$ ). There are no statistical differences between SWS latencies and the occurrence time of IPs of cerebral HHb ( $P = 0.067$ , but very close to 0.05) and BV ( $P = 0.28$ ). Significant correlation can also be found between SWS latencies and the occurrence time of IPs of HHb ( $r^2 = 0.611$ ,  $P = 0.035$ ), and the occurrence time of IPs of HbO<sub>2</sub> and HHb ( $r^2 = 0.913$ ,  $P < 0.001$ ).

Considering that the occurrences of IPs are before SWS, the reverse of cerebral HbO<sub>2</sub>, BV, and HHb changes should happen during later phase of N2, which could account for why there is no significant increment in cerebral BV from N2 to SWS shown in the previous section. Therefore, we used the amplitude values of BV at IPs to replace the mean values during N2 and repeated one-way repeated-measures ANOVA with

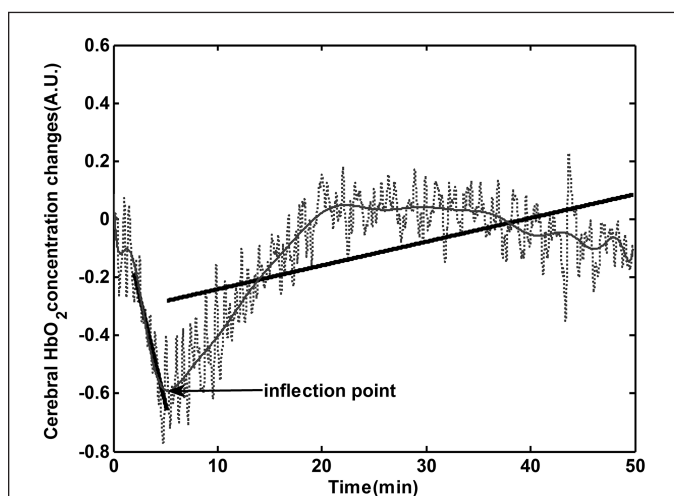


**Figure 2**—Identification of inflection point (IP) of cerebral oxygenated hemoglobin (HbO<sub>2</sub>). The dashed line is the raw HbO<sub>2</sub> changes, and the gray line represents the fitted changing trend of raw data with polynomial curve fitting method (degree = 20). Inflection point is the nadir of the fitting curve. The two black lines linearly fit the raw data before and after inflection point.

LSD *post hoc* test ( $P < 0.05$ ). We found significant main effect ( $F(3,36) = 7.29$ ,  $P = 0.013$ ), and significant increment from IPs to SWS ( $P < 0.001$ ).

### The Slopes of Linearly Fitting Lines before and after Inflection Points of Cerebral NIRS Signals

The changes of cerebral HbO<sub>2</sub> before (from the start point of N1 to IPs) and after IPs are fitted linearly, as shown in Figure 2. The slopes of the fitting lines in all subjects are listed in Table 1. Negative slope values before IPs indicate decreased hemodynamic changes, whereas subsequent increments result in a positive slope value. Before IPs, significant correlations were only observed between the slopes of HbO<sub>2</sub> and BV changes ( $r^2 = 0.57$ ,  $P = 0.038$ ), not between the slopes of HbO<sub>2</sub> and HHb ( $r^2 = 0.05$ ,  $P = 0.88$ ). However, after IPs the slope of HbO<sub>2</sub> is correlated to both BV ( $r^2 = 0.67$ ,  $P = 0.01$ ) and HHb ( $r^2 = -0.76$ ,  $P = 0.01$ ).

Moreover, initial negative slope values of BV before IPs inversely correlate with the subsequent (i.e., after IPs) positive slopes of HbO<sub>2</sub> ( $r^2 = -0.66$ ,  $P = 0.014$ ) and negative slopes of HHb ( $r^2 = 0.83$ ,  $P = 0.001$ ); and the strong correlation is also observed between the initial negative slopes of HbO<sub>2</sub> before IPs and the negative slopes of HHb after IPs ( $r^2 = 0.73$ ,  $P = 0.008$ ), but not between the slopes of HbO<sub>2</sub> before and after IPs ( $r^2 = -0.35$ ,  $P = 0.25$ ). In other words steeper initial drop in BV and HbO<sub>2</sub> are accompanied by faster subsequent HHb decrement during SWS.

### DISCUSSION

In the current study we measured cerebral and muscular hemodynamics during nocturnal sleep onset and observed characteristic changes in healthy subjects. We combined EEG and NIRS because these techniques are explicitly suitable for continuous recordings with a high temporal resolution to characterize changes of brain activity and cerebral perfusion. Compared to wakefulness we found a gradual decline in cerebral HbO<sub>2</sub> and BV but an increase in cerebral HHb after entering

**Table 1**—The occurrence time of inflection points in cerebral hemodynamic parameters, and the slopes of linearly fitting lines before and after inflection points.

Subjects	HbO <sub>2</sub> IP (min)	HbO <sub>2</sub> Slope 1	HbO <sub>2</sub> Slope 2	HHb IP (min)	HHb Slope 1	HHb Slope 2	BV IP (min)	BV Slope 1	BV Slope 2
No. 1	6.97	-0.062	0.012	6.75	0.055	-0.004	7.08	-0.051	0.014
No. 2	6.65	-0.017	0.042	—	—	—	6.87	-0.101	0.002
No. 3	8.45	-0.041	0.026	13.37	0.040	-0.010	7.13	-0.060	0.026
No. 4	7.32	-0.061	0.007	6.55	0.002	-0.006	7.63	-0.083	0.007
No. 5	5.17	-0.150	0.008	4.80	0.079	-0.005	22.57	-0.025	0.025
No. 6	3.83	-0.129	0.036	3.73	0.148	-0.022	6.53	-0.122	0.008
No. 7	8.50	-0.046	0.017	9.73	0.099	-0.012	5.15	-0.008	0.010
No. 8	3.35	-0.033	0.026	2.50	0.027	-0.002	3.20	-0.020	0.029
No. 9	13.33	-0.049	0.015	11.53	0.014	-0.019	12.10	-0.066	0.007
No. 10	3.85	-0.219	0.081	5.00	-0.018	-0.122	3.88	-0.220	0.048
No. 11	8.50	-0.036	0.061	7.02	0.067	-0.013	8.50	-0.031	0.061
No. 12	13.63	-0.004	0.037	14.92	0.059	-0.011	6.00	-0.101	0.039
No. 13	13.83	-0.044	0.023	14.88	0.028	-0.031	12.42	-0.044	0.018

Slope 1 and Slope 2 represent the slopes of linearly fitting lines before and after IPs, respectively. Dashes mean no IPs was found in subject No. 2 in the second row. BV, blood volume; HbO<sub>2</sub>, oxygenated hemoglobin; HHb, deoxygenated hemoglobin; IP, inflection point.

into light sleep (N1 and N2). With further progression from N2 to SWS, the initial declines of BV and HbO<sub>2</sub> begin to increase during SWS accompanied by a drop in HHb. By contrast, in muscle only BV significantly increases after the initiation of sleep, whereas both HbO<sub>2</sub> and HHb remain unchanged followed by a profound increase of HbO<sub>2</sub> and BV accompanied by a decline in HHb after entering into SWS. The nadirs (IPs) of cerebral HbO<sub>2</sub> and HHb occur earlier than the initiation of SWS, and their occurrence times are correlated with the latencies of SWS. We also found correlations between the slopes of cerebral BV and HbO<sub>2</sub> changes before and after IPs, whereas cerebral HbO<sub>2</sub> and HHb only correlated after IPs. Because of neurovascular coupling, changes in brain metabolism and brain perfusion induce typical patterns of concentration changes in HbO<sub>2</sub>, HHb, and BV. Our findings therefore provide several novel insights into hemodynamics and mechanisms of sleep onset. We are able to identify a biphasic time course of cerebral metabolism and BV changes and propose that these two phases likely represent two distinct processes involved in the process of sleep onset.

### **Hemodynamic Changes Mirror the Regulatory Mechanisms in Sleep**

The increasing muscular BV under the relative constant HbO<sub>2</sub> and HHb changes after entering N1 and N2 suggests that muscular blood perfusion increases without significant metabolism changes. We argue that increasing muscular perfusion is probably due to increased vasodilatation,<sup>17</sup> which promotes sleep propensity by increasing distal and proximal temperature to facilitate heat loss.<sup>3,17,28</sup> The increase in muscular BV immediately after entering N1 is in line with the results of previous studies claiming that thermoregulatory changes actually start prior to sleep stage N2.<sup>28</sup> The persistent increments of muscular BV and HbO<sub>2</sub> during SWS further fit well with previous data revealing that distal skin temperature keeps increasing to peak after about 1 h entering into sleep.<sup>17</sup>

In the brain we found clear and reliable differences compared to muscle hemodynamics implicating more complex and specific mechanisms underlying cerebral hemodynamic regulation. We can identify two phases: Phase I (before IPs) and Phase II (after IPs mainly during SWS). In Phase I the decline of cerebral BV and HbO<sub>2</sub>, together with the increase of HHb, suggest reduced cerebral metabolism. Decreased metabolic rate after entering non-rapid eye movement (NREM) sleep has been shown by previous studies,<sup>2,6</sup> and is consistent with the idea that sleep is initiated on the declining portion of the circadian rhythm of the core temperature.<sup>3,17,28</sup> Although our data are in line with these studies we extend these results by showing that this initial phase of reduced hemodynamics is followed by increased cerebral BV (Phase II), probably due to vasodilatation. In Phase II the declining cerebral HbO<sub>2</sub> and BV turn to increase, suggesting an increasing cerebral perfusion in SWS. By contrast, previous studies reported that CBF velocity continues to decrease after falling asleep until SWS,<sup>8,9</sup> and some studies argued that the cerebral perfusion may be compromised by increasing skin perfusion during sleep.<sup>3</sup> We suggest that these results should be treated with caution because velocity can only be used as an index of flow under constant vessel diameter,<sup>10</sup> but our recent study found that vasomotor activity in prefrontal

cortex changes in different sleep stages.<sup>19</sup> It is thus unlikely that the decreasing blood supply to the brain during sleep initiation can persist throughout SWS given that the brain has the highest priority in blood supply compared to other organs.<sup>29</sup> Interestingly, relative PET-CBF studies reported decreasing CBF in frontal lobe from stage N2 to SWS,<sup>6</sup> but absolute PET-CBF measurements found no decrement of CBF in cortex and suggested that relative CBF analysis may fail to estimate actual CBF changes during sleep.<sup>7</sup> In our study, we did not find a significant difference between the mean values of BV in N2 and SWS as shown in Figure 1, which confirms the result of absolute PET-CBF measurement.<sup>7</sup> High temporal resolution NIRS measurements, however, allow us to identify an increasing trend in BV and HbO<sub>2</sub> from N2 to SWS in prefrontal cortex by characterizing changes of their slope that are essentially missing in low temporal resolution PET measures.<sup>5-7</sup> Studies using event-related fMRI that can dynamically characterize the cerebral hemodynamics with similar temporal resolution as NIRS also showed increased blood-oxygen-level dependent (BOLD) signal in prefrontal area during SWS.<sup>4</sup> We argue that increasing trend in cerebral BV in Phase II is best explained by increasing vasodilatation given the declining CBF velocity. PaCO<sub>2</sub> is a potential general factor to trigger the increased vasodilatation, because sleep related hypoventilation and subsequent increases in PaCO<sub>2</sub> become stable when steady SWS is obtained.<sup>30</sup> Other potential vasodilators include sleep regulatory substances (i.e., nitric oxide[NO], adenosine, interleukin-1, growthhormone-releasing hormone, tumor necrosis factor, and prostaglandins),<sup>14,15</sup> and modulation of neurotransmitters including inhibitors of the adrenergic system, such as calcitonin gene-related peptide.<sup>2,31</sup>

Our data further suggest that cerebral hemodynamic change during sleep initiation is brain specific in contrast to muscular hemodynamics. Of note, the slopes of cerebral BV and HbO<sub>2</sub> correlate in both phases but the ones of HbO<sub>2</sub> and HHb only correlate in Phase II, indicating a mismatch between oxygenation and blood supply in Phase I.<sup>32</sup> Therefore, we reason that cerebral hemodynamics in Phases I and II can represent different regulatory mechanisms during sleep because they are characterized by different temporal cerebral perfusion/oxygenation patterns and by correlated ('matched')/uncorrelated ('mismatched') slopes of hemodynamic parameters.

### **The Occurrence of IPs and Functional Implications of Increased Cerebral BV in SWS**

Our finding that the IPs of HbO<sub>2</sub> and HHb occur earlier and correlate with the latencies of SWS is remarkable. As outlined previously, vasodilatation may counterbalance initial decline of BV in the brain. Such a counterregulation may be accomplished by cerebral vascular autoregulation<sup>2,29</sup> and could reflect a protective role to prevent the further decline of cerebral blood supply in Phase I. Increased cerebral BV is a prerequisite for metabolite clearance, which manipulates the influx of cerebrospinal fluid and interstitial fluid during sleep.<sup>31,33</sup> A recent study by Xie et al. found that influx of cerebrospinal fluid and the volume of the extracellular space in cortex strongly increased during sleep compared to wakefulness in mice, resulting in improvement of clearance of  $\beta$ -amyloid in the interstitial space surrounding neurons.<sup>31</sup> Taking the conclusions from Xie's

study into account, the increased BV in SWS may play a crucial role in cleaning potentially neurotoxic waste products that accumulate during wakefulness.<sup>31</sup> The increased vasodilatation and cerebral BV can also provide increased oxidative substrate supply to cortical tissues, which may indicate a protective role of SWS in preventing pathological neurovascular events such as spreading depolarization, which is accompanied by severe vasoconstriction in patients with stroke and brain trauma.<sup>1,19,34</sup>

### Limitations and Perspective in the Future

Several limitations in our study need further investigations. First, we did not measure temperature changes so we can only refer to the literature to interpret the cerebral and peripheral hemodynamic changes. Adding core and peripheral temperature measurements in the future can provide more profound insights into the interaction of sleep and thermoregulation systems and highlight the role of blood in metabolism and thermoregulation. Second, we cannot clarify the mechanisms responsible for inducing IPs but propose vasodilators (e.g., PaCO<sub>2</sub>, NO, etc.) as candidate mediators. Whether the occurrence time of both IPs and SWS latency can be modulated by these vasodilators at the same time would be an interesting topic for future studies investigating sleep regulation system and pathological mechanisms of sleep disorders such as insomnia and sleep apnea.

Third, SWS in our study was scored from conventional all-night PSG measurements with limited spatial information of EEG, meaning it reflects global low-frequency synchronization of neural activity.<sup>35</sup> Previous studies have suggested that the process of falling asleep is a progressive generation of slow waves confined to a few local cortical areas and then became more and more globally synchronous.<sup>36</sup> The neural circuitries underlying homeostatic sleep regulation are still poorly understood. Cortical type I sleep-active NO synthase neurons distributed throughout all cortical areas have been suggested to be involved in homeostatic sleep process and their activation during sleep is restricted to the cortex.<sup>14,37</sup> Recently, some evidence also indicated that sleep might be regulated at a local network level (i.e., individual neural assemblies such as cortical columns<sup>15,38</sup>) and the local slow wave induction is daytime use-dependent.<sup>15,39</sup> A prefrontal predominance of slow wave activity during NREM sleep has been reported in EEG studies.<sup>40</sup> NIRS can measure local cortical hemodynamics in macroscopic (~1–10 cm<sup>3</sup>) tissue volumes<sup>41</sup> and the light penetration depth is more than 2 cm (under 4 cm light source to sensor distance).<sup>18,27</sup> Therefore, we believe that NIRS can measure hemodynamics of numbers of local prefrontal cortical columns modulated by sleep. The IPs of local hemodynamics occurring before global SWS may be a hemodynamic marker of local SWS in the measured cortex. Further studies conducting high-density EEG and whole brain NIRS measurements are needed to further test whether local SWS in specific cortical area can induce similar local hemodynamic changes as shown in this study.

Fourth, the importance of intraparenchymal vessels in neurovascular coupling via their anatomical and functional connections to astrocytes has been recognized recently.<sup>29,42</sup> The information NIRS measured comes from both pial arteries and intraparenchymal vessels,<sup>18,27,41</sup> so we cannot distinguish their exact contributions (although probably mainly from

small vessels<sup>43,44</sup>; e.g., smaller arteries, arterioles, venules, and capillaries major in parenchyma). However, our data can still provide insights into neurovascular coupling during sleep. We should expect a decreasing cerebral perfusion in SWS if we follow the hypothesis of synaptic downscaling (i.e., synaptic downscaling should reduce cerebral metabolism to improve signal to noise ratio and to save energy thus decreasing cerebral perfusion).<sup>45</sup> However, we found opposite results (i.e., increasing cerebral BV) allowing us to reasonably hypothesize that the regulation of cerebral perfusion during sleep does not simply depend on neuronal metabolic activity alone, but also relies on other mechanisms such as glial and astrocyte control of transmitters (e.g., NO and adenosine).<sup>29,46</sup>

### CONCLUSION

We found that the hemodynamic changes in cerebral and muscular tissues show distinct changing patterns after falling asleep. Of note, our result of increasing cerebral BV in prefrontal cortex from N2 to SWS does not contradict the decreasing CBF reported by previous studies<sup>2,5–7,9</sup> because essentially CBF is not equal to cerebral BV,<sup>47</sup> but provides evidence showing that the amount of cerebral blood increases in SWS. As we can reasonably attribute the increasing BV to vasodilatation, our data can fill in the gap between previous results on CBF, PaCO<sub>2</sub>, neurotransmitters, and recent studies on vasodilatation. Thus, providing cerebral and muscular BV changes will be helpful to improve our knowledge of sleep regulation mechanisms.

### ACKNOWLEDGMENTS

The authors are grateful to Professor Martin Wolf for his support on the NIRS technique. We thank the technicians from Center for Sleep Medicine and Sleep Research at Clinic Barmelweid for their technical supports.

### DISCLOSURE STATEMENT

This was not an industry supported study. This work was supported by Clinic Barmelweid Scientific Foundation. This work was performed in the Center for Sleep Medicine and Sleep Research, Clinic Barmelweid, Switzerland. Dr. Khatami has participated in speaking engagements for UCB and has received research support from ResMed. Dr. Zhang has received research support from ResMed.

### REFERENCES

1. Dreier JP. The role of spreading depression, spreading depolarization and spreading ischemia in neurological disease. *Nat Med* 2011;17:439–47.
2. Maquet P. Functional neuroimaging of normal human sleep by positron emission tomography. *J Sleep Res* 2000;9:207–31.
3. Van Someren EJ. Mechanisms and functions of coupling between sleep and temperature rhythms. *Prog Brain Res* 2006;153:309–24.
4. Dang-Vu TT, Schabus M, Desseilles M, et al. Spontaneous neural activity during human slow wave sleep. *Proc Natl Acad Sci U S A* 2008;105:15160–5.
5. Braun AR, Balkin TJ, Wesenten NJ, et al. Regional cerebral blood flow throughout the sleep-wake cycle. An H<sub>2</sub>(15)O PET study. *Brain* 1997;120:1173–97.
6. Hofle N, Paus T, Reutens D, et al. Regional cerebral blood flow changes as a function of delta and spindle activity during slow wave sleep in humans. *J Neurosci* 1997;17:4800–8.

7. Kajimura N, Uchiyama M, Takayama Y, et al. Activity of midbrain reticular formation and neocortex during the progression of human non-rapid eye movement sleep. *J Neurosci* 1999;19:10065–73.
8. Meadows GE, O'Driscoll DM, Simonds AK, Morrell MJ, Corfield DR. Cerebral blood flow response to isocapnic hypoxia during slow-wave sleep and wakefulness. *J Appl Physiol* 2004;97:1343–8.
9. Klingelhofer J, Hajak G, Matzander G, et al. Dynamics of cerebral blood flow velocities during normal human sleep. *Clin Neurol Neurosurg* 1995;97:142–8.
10. Barnes JN. Beyond a one-track mind: understanding blood flow to the brain in humans. *J Physiol* 2012;590:3217.
11. Ito H, Kanno I, Ibaraki M, Hatazawa J, Miura S. Changes in human cerebral blood flow and cerebral blood volume during hypercapnia and hypocapnia measured by positron emission tomography. *J Cereb Blood Flow Metab* 2003;23:665–70.
12. Willie CK, Macleod DB, Shaw AD, et al. Regional brain blood flow in man during acute changes in arterial blood gases. *J Physiol* 2012;590:3261–75.
13. Naifeh KH, Kamiya J. The nature of respiratory changes associated with sleep onset. *Sleep* 1981;4:49–9.
14. Pasumarthi RK, Gerashchenko D, Kilduff TS. Further characterization of sleep-active neuronal nitric oxide synthase neurons in the mouse brain. *Neuroscience* 2010;169:149–57.
15. Krueger JM, Rector DM, Roy S, Van Dongen HP, Belenky G, Panksepp J. Sleep as a fundamental property of neuronal assemblies. *Nat Rev Neurosci* 2008;9:910–9.
16. Raymann RJ, Swaab DF, Van Someren EJ. Skin deep: enhanced sleep depth by cutaneous temperature manipulation. *Brain* 2008;131:500–13.
17. Krauchi K, Cajochen C, Werth E, Wirz-Justice A. Functional link between distal vasodilation and sleep-onset latency? *Am J Physiol Regul Integr Comp Physiol* 2000;278:R741–8.
18. Scholkmann F, Kleiser S, Metz AJ, et al. A review on continuous wave functional near-infrared spectroscopy and imaging instrumentation and methodology. *Neuroimage* 2014;85:6–27.
19. Zhang Z, Khatami R. Predominant endothelial vasomotor activity during human sleep: a near-infrared spectroscopy study. *Eur J Neurosci* 2014;40:3396–404.
20. Zhang Z, Schneider M, Fritschi U, Lehner I, Khatami R. Near-infrared spectroscopy (NIRS) as a useful tool to evaluate the treatment efficacy of positive airways pressure therapy in patients with obstructive sleep apnea syndrome (OSAS): a pilot study. *J Innov Opt Health Sci* 2014;7:1450014.
21. Pizza F, Biallas M, Kallweit U, Wolf M, Bassetti CL. Cerebral hemodynamic changes in stroke during sleep-disordered breathing. *Stroke* 2012;43:1951–3.
22. Hoshi Y, Mizukami S, Tamura M. Dynamic features of hemodynamic and metabolic changes in the human brain during all-night sleep as revealed by near-infrared spectroscopy. *Brain Res* 1994;652:257–62.
23. Spielman AJ, Zhang G, Yang CM, et al. Intracerebral hemodynamics probed by near infrared spectroscopy in the transition between wakefulness and sleep. *Brain Res* 2000;866:313–25.
24. Saager RB, Telleri NL, Berger AJ. Two-detector Corrected Near Infrared Spectroscopy (C-NIRS) detects hemodynamic activation responses more robustly than single-detector NIRS. *Neuroimage* 2011;55:1679–85.
25. Iber C, Ancoli-Israel S, Chesson A, Quan SF. *The AASM Manual for the Scoring of Sleep and Associated Events: Rules, Terminology and Technical Specifications*. 1st ed. Westchester, IL: American Academy of Sleep Medicine, 2007.
26. Suzuki S, Takasaki S, Ozaki T, Kobayashi Y. A tissue oxygenation monitor using NIR spatially resolved spectroscopy. *Proc SPIE* 1999;3597.
27. Firbank M, Okada E, Delpy DT. A theoretical study of the signal contribution of regions of the adult head to near-infrared spectroscopy studies of visual evoked responses. *Neuroimage* 1998;8:69–78.
28. Krauchi K. The human sleep-wake cycle reconsidered from a thermoregulatory point of view. *Physiol Behav* 2007;90:236–45.
29. Iadecola C, Nedergaard M. Glial regulation of the cerebral microvasculature. *Nat Neurosci* 2007;10:1369–76.
30. Trinder J, Whitworth F, Kay A, Wilkin P. Respiratory instability during sleep onset. *J Appl Physiol* 1992;73:2462–9.
31. Xie L, Kang H, Xu Q, et al. Sleep drives metabolite clearance from the adult brain. *Science* 2013;342:373–7.
32. Cui X, Bray S, Reiss AL. Functional near infrared spectroscopy (NIRS) signal improvement based on negative correlation between oxygenated and deoxygenated hemoglobin dynamics. *Neuroimage* 2010;49:3039–46.
33. Dickstein JB, Hay JB, Lue FA, Moldofsky H. The relationship of lymphocytes in blood and in lymph to sleep/wake states in sheep. *Sleep* 2000;23:185–90.
34. Poryazova R, Huber R, Khatami R, et al. Topographic sleep EEG changes in the acute and chronic stage of hemispheric stroke. *J Sleep Res* 2015;24:54–65.
35. Vyazovskiy VV, Harris KD. Sleep and the single neuron: the role of global slow oscillations in individual cell rest. *Nat Rev Neurosci* 2013;14:443–51.
36. Deco G, Hagmann P, Hudetz AG, Tononi G. Modeling resting-state functional networks when the cortex falls sleep: local and global changes. *Cereb Cortex* 2014;24:3180–94.
37. Morairty SR, Dittrich L, Pasumarthi RK, et al. A role for cortical nNOS/NK1 neurons in coupling homeostatic sleep drive to EEG slow wave activity. *Proc Natl Acad Sci U S A* 2013;110:20272–7.
38. Krueger JM, Huang YH, Rector DM, Buysse DJ. Sleep: a synchrony of cell activity-driven small network states. *Eur J Neurosci* 2013;38:2199–209.
39. Huber R, Ghilardi MF, Massimini M, Tononi G. Local sleep and learning. *Nature* 2004;430:78–81.
40. Tinguely G, Finelli LA, Landolt HP, Borbely AA, Achermann P. Functional EEG topography in sleep and waking: state-dependent and state-independent features. *Neuroimage* 2006;32:283–92.
41. Fantini S. Dynamic model for the tissue concentration and oxygen saturation of hemoglobin in relation to blood volume, flow velocity, and oxygen consumption: implications for functional neuroimaging and coherent hemodynamics spectroscopy (CHS). *Neuroimage* 2014;85:202–21.
42. Petzold GC, Murthy VN. Role of astrocytes in neurovascular coupling. *Neuron* 2011;71:782–97.
43. Liu H, Chance B, Hielscher AH, Jacques SL, Tittel FK. Influence of blood vessels on the measurement of hemoglobin oxygenation as determined by time-resolved reflectance spectroscopy. *Med Phys* 1995;22:1209–17.
44. Kurth CD, Steven JM, Nicolson SC. Cerebral oxygenation during pediatric cardiac surgery using deep hypothermic circulatory arrest. *Anesthesiology* 1995;82:74–82.
45. Tononi G, Cirelli C. Sleep function and synaptic homeostasis. *Sleep Med Rev* 2006;10:49–62.
46. Halassa MM, Florian C, Fellin T, et al. Astrocytic modulation of sleep homeostasis and cognitive consequences of sleep loss. *Neuron* 2009;61:213–9.
47. Grandin CB, Bol A, Smith AM, Michel C, Cosnard G. Absolute CBF and CBV measurements by MRI bolus tracking before and after acetazolamide challenge: repeatability and comparison with PET in humans. *Neuroimage* 2005;26:525–35.